HPC4EnergyInnovation Final Report

Project Title: Efficient and Safe Hydrogen Refueling of Fuel Cell Vehicles from an Emergency Chemical Hydride Storage Source

Short Project Description: To assuage fears of fuel cell vehicle owners running out of hydrogen fuel, an emergency hydrogen refueler that can be stored in the vehicle's trunk was developed. This refueler contains lithium hydride (LiH). Once activated with water, LiH releases hydrogen gas, thereby refilling the vehicle with sufficient emergency fuel to travel 50 miles to a hydrogen refueling station. Advanced modeling and experiments of the reactor that account for spatial and temporal variations of heat and mass transfer, along with variable reaction rates, were performed to improve refueler performance.

Company Name: Skyhaven Systems, LLC.

Company Sector: Defense, Energy, Aerospace, and Environmental

Process Category: Research and Development firm

Proposal ID: DE-NA0003525

HPC4EI Program (HPC4Mfg or HPC4Mtls): HPC4Mtls

CRADA Agreement ID: SV18/01935.00

MPO ID (if applicable):

Approved/Costed Budget: $300k

Principal Investigator (PI) Contact Information (include all co-PIs)

Name: Michael C. Kimble, PhD

Company/Division: Skyhaven Systems, LLC

Title: President and Founder, Skyhaven Systems, LLC

Nationality: U.S.

Address: 405 S. Lincoln Avenue, Suite B209,

Steamboat Springs, CO 80487

Phone number: (970)846-0547

Email address: mkimble@skyhavensystems.com

Name: Daniel R. Carr, PhD

Company/Division: Skyhaven Systems, LLC

Title: Vice President-Operations and Research Engineer, Skyhaven

Nationality: U.S.

Address: 2 Park Drive, Unit 4, Westford, MA 01886

Phone number: (978)692-4664

Email address: dcarr@skyhavensystems.com

National Laboratory PI Contact Information

Name: Gabriela Bran Anleu, PhD

Laboratory: Sandia National Labs

Email: gabrana@sandia.gov

Phone number: (925)6670282

Computational Resources used for Project:

System	Time (MCH)	Largest # of cores used	Commercial Software	Custom Software
HPC clusters		72	-	Sierra:Aria

Briefly describe any algorithm development. How and to what extent will this development be disseminated internally and/or externally?

The hydrogen refueler was modeled using the Aria multi-physics module from Sandia's SIERRA mechanics simulation code suite. The model consists of a two-dimensional (2D) axisymmetric porous media reacting two-phase flow system. The Van Genuchten saturation model [1, 2] in Aria was used to calculate the saturation in the domain. This model had significant limitations in the regions where the liquid saturation is close to zero. As the liquid saturation approaches to zero, the Van Genuchten model for capillary pressure approaches infinity. The Aria solvers failed to converge to a solution once liquid saturation was close to zero. The low saturation regime is important in the hydrogen refueler, because the refueler is initially filled only with air, so the liquid saturation is zero. As liquid water enters the domain, it quickly reacts with LiH. The liquid saturation remains close to zero until most of the LiH has reacted. In order to overcome this limitation, the developers at SNL incorporated into Aria the extension to the Van Genuchten equation developed by Webb [3]. This simple extension of the saturation curves retains the fit at higher saturations obtained by the Van Genuchten equation and improves the fit at lower saturations.

Another novel and extended capability in Aria was the addition of an energy equation for open systems that solves for only one temperature by assuming that the solid, liquid, and gas species are

at the same temperature. Aria can already solve for one temperature using the porous energy equation for closed systems. However, the hydrogen refueler has an open boundary condition where the gas is able to leave the domain, which Aria could not handle before this project. SNL developers extended the main Aria code to allow for an open boundary condition.

Aria can solve for the fluxes at the boundary conditions using the residuals for the partial differential equations being solved. This capability had been extensively used in 3-dimensional (3D) problems. However, it had not been used in 2D axisymmetric problems. While working on the hydrogen refueler, a bug was found in the calculation of the fluxes at the boundary for axisymmetric problems. This bug was fixed and tested with the hydrogen refueler model.

SNL validated the model against experimental data produced by Skyhaven. In addition, SNL expanded Sierra's material property library with data provided by Skyhaven.

SNL will use all the new capabilities added as part of the hydrogen refueler project in other projects that deal with similar physics, such as thermal batteries, material decomposition, and geothermal systems.

Executive Summary

Zero-emissions hydrogen fuel cell electrical vehicles (FCEVs) have become more popular in recent years. However, the limited availability of hydrogen fueling stations is considered a critical barrier to sustainable adoption of hydrogen FCEV. To enable the widespread deployment and commercialization of hydrogen FCEV, the availability of hydrogen refueling stations needs to improve. One of the consequences of the lack of hydrogen refueling infrastructure is that consumers can suffer from "range anxiety", meaning consumers would get anxious of running out of fuel during long-distance trip [4]. A practical solution is to provide a compact emergency hydrogen refueler that can be used if the consumer runs out of hydrogen before reaching the nearest hydrogen refueling station. A safe, compact, and user-friendly hydrogen refueler would give consumers the flexibility they need to feel comfortable using their hydrogen FCEV when planning a long-distance trip. Offering this product would alleviate range anxiety, and it would make Hydrogen FCEV a more attractive alternative to gasoline vehicles. The emergency hydrogen refueler consists of a lithium hydride bed that reacts with liquid water to produce hydrogen gas and lithium hydroxide.

This project brought the emergency refueler a step closer to commercialization. Skyhaven will use the findings of this project to improve their emergency refueler. A peer-reviewed journal paper will be published with all the findings of this work. Additionally, Sandia improved the Multiphysics models of complex systems such as the refueler studied here. SNL validated the model against experimental data produced by Skyhaven. SNL can now use this type of model for projects that deal with similar physics, such as thermal batteries. In addition, SNL was able to expand Sierra's material property library with data provided by Skyhaven.

This emergency hydrogen refueler supports the DOE Fuel Cell Technologies Office (FCTO) goal of advancing hydrogen and fuel cells for transportation by contributing to the U.S. energy independence, security and resiliency, and adds to a strong domestic economy. Offering this emergency hydrogen refueler to vehicle owners will help alleviate range anxiety, further helping to commercialize hydrogen fuel cell vehicles and the continuing commissioning of hydrogen refueling stations. This project will help drive the growth of both fuel cell vehicles and hydrogen refueling stations by offering an emergency hydrogen refueling option to consumers. This project supports the nation's energy strategy by helping to diversify America's energy sector, reducing the dependence on foreign oil, and reducing petroleum combustion emissions by accelerating the deployment of fuel cell vehicle technologies. The hydrogen refueler will greatly reduce barriers to market penetration by allowing hydrogen fuel cell vehicle users to have an extended driving range in case of emergency due to a lack of hydrogen refueling stations.

Introduction

Problem Description and Motivation

The emergency hydrogen refueler consists of a lithium hydride bed that reacts with liquid water to produce hydrogen gas and lithium hydroxide. A schematic of the hydrogen refueler is shown in Figure 1. The hydrogen refueler consists of a cylindrical conduit filled with LiH powder. The conduit wall is fabricated using a polymeric membrane with a 50% sulfonation, which allows liquid water to permeate through the conduit wall. The outer wall of the conduit is surrounded by liquid water at ambient pressure and temperature. Liquid water permeates through the conduit wall and immediately reacts with LiH particles to produce hydrogen gas and LiOH according to Equation (1). Reaction (1) is an exothermic reaction which causes the temperature inside of the bed to increase. Under certain combinations of the water inlet flux and initial hydride content, the heat from Reaction (1) can cause liquid water vaporization according to Equation (3). Water vapor also reacts with LiH to generate hydrogen gas and LiOH, according to Equation (2).

$$LiH_{(s)} + H_2O_{(l)} \rightarrow LiOH_{(s)} + H_{2(g)} \quad (1)$$

$$LiH_{(s)} + H_2O_{(g)} \rightarrow LiOH_{(s)} + H_{2(g)} \quad (2)$$

$$H_2O_{(l)} \rightarrow H_2O_{(g)} \quad (3)$$

Although there are several advantages to using LiH as a hydrogen storage material, there are two main challenges to designing a safe, light weight, and compact hydrogen refueler. The first challenge is to control the reaction rate and temperature increase in the bed, especially when liquid water (instead of vapor) is being used to react with LiH [5]. The hydrolysis of lithium hydride is an exothermic reaction, thermal management is required for the system to function safely. Kong et.al. [5] observed extremely rapid reactions rates and rapid temperature increases on a LiH bed when liquid water was introduced. The authors showed that the reaction rate and heat release can be controlled by limiting the amount of water fed into the chemical hydride bed and by dispersing the water over a larger area within the bed to prevent hotspots. Unfortunately, in order to meet the target hydrogen production rate for the refueler, higher water flow rates are needed. In addition, larger lithium hydride beds complicate the design objectives of a compact and light weight refueler.

The second challenge is the formation of the LiOH-H_2O film at the reaction interface. Several authors noticed a reduction of hydrogen produced due to the rapid formation of a LiOH-H_2O film. After this layer forms, water can only penetrate the rest of the LiH material by diffusion though cracks in the film [6, 7]. If not all the LiH reacts with water, the refueler would need to be heavier and larger to be able to produce the same amount of hydrogen that a refueler that can achieve 100 % reaction would.

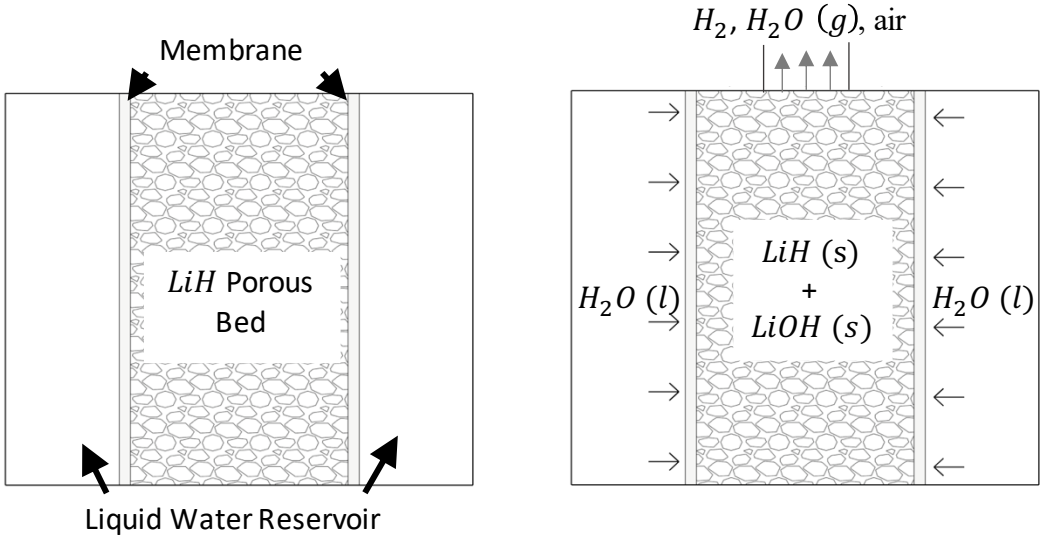

Figure 1: Schematic of water permeation through membrane into the LiH porous bed.

In order to address these two main challenges, a numerical model was developed to investigate the design parameters and to improve the hydrogen generation and thermal management of the reaction. In this project, a lithium hydride porous bed that reacts with water to produce hydrogen was simulated using a two-dimensional multiphysics model. As shown in Figure 2, the model does not include the membrane or the water reservoir; it only includes the LiH bed. The numerical model was validated with experimental results obtained at the Skyhaven laboratory. A parametric study was performed to determine ways to improve the design of the refueler. The parameters that varied from a reference case were: 1) the initial temperature of the LiH bed, 2) the inlet temperature of the liquid water, 3) the diameter of the bed, 4) the length of the bed , and 5) the initial mass of lithium hydride. For the cases where the diameter and length were varied, two density subcases were explored. The first case used a constant porosity and varied the initial LiH mass, while the second case fixed a constant initial LiH mass and varied the porosity.

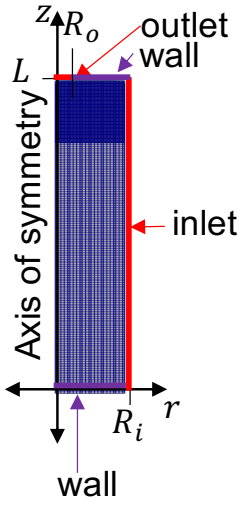

Figure 2: Numerical domain 2D axisymmetric domain for numerical simulation.

Project Approach

Sandia developed and incorporated the physical and transport properties obtained by Skyhaven into a Multiphysics model that solves the highly coupled equations that describe the hydrogen generation process, namely the mass, energy, flow, and reaction rate equations.

Material Models

Kinetics

The net rate of change of density of species i , summed over all j reactions is expressed as,

$$\frac{\partial \rho_i}{\partial t} = \omega_i''' = \sum_{j=1}^{N_r} \left(\nu_{ij}'' - \nu_{ij}'\right) r_j \tag{4}$$

where N_r is the number of reactions, υ_{ij}'' is the mass-based stoichiometric coefficient for the product species and υ_{ij}' is the mass-based stoichiometric coefficient for the reactant species. The mass base reaction rate, r_j, is calculated according to the law of mass action,

$$r_j = k_j M_{ref} \prod_{i=1}^{N_s} \rho_i^{\mu_{ij}} \tag{5}$$

where M_{ref} is the molecular weight of the reference species, N_s is the number of species i, μ_{ij} is the concentration exponent for species in reaction j. The kinetic coefficient, k_j, for reaction j is modeled using the Arrhenius form,

$$k_j = A_j exp\left(-\frac{E_j}{RT}\right) \tag{6}$$

where A_j is the pre-exponential factor, and E_j is the activation energy of reaction j. R is the universal gas constant, and T is the temperature.

The overall mass-based continuity equation source term for material phase k was computed as the summation of all the individual species source terms,

$$\omega_{c,k}''' = \frac{\partial \rho_k}{\partial t} = \sum_{i=1}^{N_{s,k}} \frac{\partial \rho_i}{\partial t} \tag{7}$$

Evaporation

$$H_2O_{(l)} \rightarrow H_2O_{(g)} \tag{8}$$

The phase change of water was assumed to be a finite rate derived from the difference between the local thermodynamic state and the equilibrium state [8, 9]. The first term in Eq. *(9)* is the rate of evaporation of liquid water, and the second term is the condensation rate of water vapor,

$$r_{H_2O} = \begin{cases} M_l \kappa_c \dfrac{\phi x_{H_2O,g}}{RT}\left(x_{H_2O,g} p_g - p_{sat}\right) & if\ x_{H_2O,g} P > P_{sat} \\ \kappa_e \phi S_l \rho_l \left(x_{H_2O,g} p_g - p_{sat}\right) & if\ x_{H_2O,g} P < P_{sat} \end{cases} \quad (9)$$

where κ_c and κ_e are the condensation and evaporation coefficients, respectively. The condensation and evaporation coefficients are given by Nguyen et. al. [10]. The partial pressure of water vapor, $x_{H_2O,g} p_g$, is calculated using the mole fraction of water vapor, $x_{H_2O,g}$, times the gas phase pressure, p_g. The saturation pressure of water, P_{sat}, is calculated using the curve-fitted expressions provided by Springer et al. [11],

$$log_{10} p_{sat} = -2.1794 + 0.02953T - 9.1837 \times 10^{-5} T^2 + 1.4454 \times 10^{-7} T^3 \quad (10)$$

where T is the temperature of the bed.

Porous Media Two-Phase Flow

The porosity, ϕ, of the porous material is defined as the ratio of the volume of pore space, V_p, and the total volume, V_t, namely

$$\phi = \frac{V_p}{V_t} = \frac{V_l + V_g}{V_l + V_g + V_s} \quad (11)$$

where V_s is the volume of the solid material, V_l is the volume occupied by the liquid phase, and V_g is the volume occupies by the gas material.

The volumetric gas saturation, S_g, is defined as the fraction of the interstitial pore space occupied by the gas phase and is calculated from the assumption that the pore space is saturated with fluids,

$$S_g + S_l = 1 \quad (12)$$

Capillary pressure, p_c, and volumetric liquid saturation, S_l, are related by the Van Genuchten Model [1, 2],

$$p_c = \frac{1}{\alpha}\left[\left(\frac{S_l - S_{lr}}{1 - S_{lr}}\right)^{-1/m} - 1\right]^{1/n} \quad for\ p_c > 0 \quad (13)$$

where S_{lr} is the residual liquid saturation and n, m and α are Van Genuchten parameters that depend on the type of porous material. The Mualem relationship [12] was used to find $m = 1 - 1/n$. The capillary pressure, p_c, is calculated from the liquid pressure p_l and the gas pressure p_g,

$$p_l = p_g - p_c \quad (14)$$

The gas and liquid phase mass average velocities are calculated using Darcy's Law [13]:

$$\boldsymbol{u}_\gamma = -\frac{\kappa_\gamma}{\mu_\gamma}\left(\frac{\partial p_\gamma}{\partial x_j} + \rho_\gamma g_j\right) \quad \gamma = l\ or\ g \quad (15)$$

where g_j is the gravity vector, κ_γ is the permeability of phase γ, and μ_γ is the viscosity of phase γ. The liquid density, ρ_l, is assumed to be constant. The gas density, ρ_g, is calculated using the ideal gas law,

$$\rho_g = \frac{p_g M_g}{RT} \tag{16}$$

where p is the gas pressure and M_g is the mass averaged molecular weight of the gaseous mixture which is calculated from the summation of the product of $Y_{i,g}$, the gas phase mass fraction of species i, and $M_{i,g}$, the molecular weight of the gas species i,

$$M_g = \sum_i Y_{i,g} M_{i,g} \tag{17}$$

Mixture Properties

The mass diffusivity for component 1 in a gas mixture is given by Welty and Wilson [14]:

$$D_{1-mixture} = \frac{1}{\frac{h_2'}{D_{1-2}} + \frac{h_3'}{D_{1-3}} + \cdots + \frac{h_n'}{D_{1-i}}} \tag{18}$$

where D_{1-i} is the mass diffusivity of the binary pair (component 1 and i), and the molar fraction of component i in a gas mixture of the binary pair is defined as

$$h_i' = \frac{h_i}{(1-h_1)} \tag{19}$$

where h_i is the molar fraction of component i in a binary mixture of component 1 and i. The diffusion coefficient for the binary pairs of non-polar, non-reacting molecules are assumed to be constant.

The tortuosity factor is calculated from the Bruggeman model [15],

$$\tau_\gamma = \frac{1}{a\phi^n} \; where \; \gamma = l \; or \; g \tag{20}$$

The diffusion coefficients are effective values modified via Bruggman correlation to account for the effects of porosity and tortuosity in porous media [16].

$$\frac{D_{eff}}{D_{1-mixture}} = \frac{\varepsilon}{\tau_\gamma} \; where \; \gamma = l \; or \; g \tag{21}$$

The Carman-Kozeny model [17-19] was used to calculate the intrinsic permeability of the porous bed,

$$k_s = \frac{1}{2{\tau_g}^2 S_v^2} \frac{\phi^3}{(1-\phi)^2} \tag{22}$$

where $S_v = d/6$ (d is the particle diameter). The relative permeability of the liquid phase is calculated using the Van Genuchten-Mualem expression [2, 12],

$$k_{r,l} = \left(\frac{S_l - S_{lr}}{1 - S_{lr}}\right)^{-1/2} \left[1 - \left(1 - \left(\frac{S_l - S_{lr}}{1 - S_{lr}}\right)^{1/m}\right)^m\right]^2 \quad (m = 1 - 1/n) \tag{23}$$

The relative permeability of the gas is calculated using the Luckner expression [20],

$$k_{r,g} = \left(1 - \frac{S_l - S_{lr}}{1 - S_{lr}}\right)^{1/3} \left(1 - \left(\frac{S_l - S_{lr}}{1 - S_{lr}}\right)^{1/m}\right)^{2m} \quad (m = 1 - 1/n) \tag{24}$$

Governing Equations

There are separate mass balance equations for the solid phase and gas phase.

Conservation of Mass

The solid phase mass balance equation is used to solve for the solid phase density, ρ_s,:

$$\frac{\partial \rho_s}{\partial t} = -\omega_g''' \tag{25}$$

where $\omega_{f,g}'''$ is the rate of formation of gases due to heterogenous reaction kinetics.

The gas density is used in the mass balance equation for the gas phase to solve for the pressure of the gas phase, P_g:

$$\frac{\partial(\phi S_g \rho_g)}{\partial t} + \frac{\partial(\rho_g u_{j,g})}{\partial x_j} = \omega_g''' \tag{26}$$

The final equation used to solve for the gas pressure is obtained by substituting the velocity, $u_{j,g}$, with Equation (15) and ρ_g with Equation (16),

$$\frac{\partial}{\partial t}\left(\phi S_g \frac{P_g M_g}{RT}\right) + \frac{\partial}{\partial x_j}\left[\left(\frac{P_g M_g}{RT}\right)\left(-\frac{\kappa_g}{\mu_g}\left(\frac{\partial P_g}{\partial x_j} + \frac{P_g M_g}{RT} g_j\right)\right)\right] = \omega_g''' \tag{27}$$

The liquid phase mass balance equation is used to calculate the pressure of the liquid phase P_l,

$$\frac{\partial(\phi S_l \rho_l)}{\partial t} + \frac{\partial}{\partial x_j}(\rho_l u_{j,l}) = \omega_l''' \tag{28}$$

The final equation used to solve for the liquid pressure is obtained by substituting for $u_{j,l}$ with Equation (15),

$$\frac{\partial(\phi S_l \rho_l)}{\partial t} + \frac{\partial}{\partial x_j}\left[\rho_l\left(-\frac{\kappa_l}{\mu_l}\left(\frac{\partial P_l}{\partial x_j} + \rho_l g_j\right)\right)\right] = \omega_l''' \tag{29}$$

Conservation of Chemical Species

The solid phase species equations solve for the solid phase mass fraction, $Y_{i,s}$, of species i,

$$\frac{\partial \rho_s Y_{i,s}}{\partial t} = \dot{\omega}_{i,s}''' \tag{30}$$

The gas phase species equations solve for the gas phase mass fraction, $Y_{i,g}$, of species i,

$$\frac{\partial(\phi S_g \rho_g Y_{i,g})}{\partial t} + \frac{\partial(\rho_g u_{j,g} Y_{i,g})}{\partial x_j} + \frac{\partial\left(q_{ij}^{Y_{i,g}}\right)}{\partial x_j} = \dot{\omega}_{i,g} \tag{31}$$

The gas-phase species diffusion flux vector $q_{ij}^{Y_{i,g}}$ is modeled as

$$q_{ij}^{Y_{i,g}} = -\phi\rho_g D_{i,g}\frac{\partial\left(Y_{i,g}\right)}{\partial x_j} \tag{32}$$

where $D_{i,g}$ is the gas-phase mass diffusivity for species i.

Conservation of Energy

The system is assumed to be in a local thermal equilibrium, so that the solid, liquid, and gas phases have a common average temperature, *T*. The energy balance equation that describes the system takes the form

$$\begin{aligned}\frac{\partial}{\partial t}\left[(1-\phi)\rho_s h_s + \phi\left(\rho_l S_l h_l + \rho_g S_g h_g\right)\right] + \frac{\partial}{\partial x_j}\left[\rho_l u_{j,l} h_l + \rho_g u_{j,g} h_g\right] \\ = -\frac{\partial q_j^h}{\partial x_j} + S_{h_s}\end{aligned} \tag{33}$$

where h_s h_l, and h_g are the enthalpy of the solid, liquid, and gas phases, respectively. The energy diffusive flux vector, $q_j^{h,g}$, is represented as

$$q_j^h = -\left(\phi\rho_l D_l\frac{\partial h_l}{\partial x_j} + \rho_g D_g\frac{\partial h_g}{\partial x_j}\right) \tag{34}$$

The source term due to the heat of reaction is

$$S_{h_s} = -\sum_{i=1}^{N_s}\Delta h_{f,i}^{\circ}\dot{\omega}_i''' \tag{35}$$

where $\Delta h_{f,i}^{\circ}$ is the mass-based heat of formation for species i at the reference temperature T_{ref}.

Initial Conditions

The LiH bed is initially filled with air at ambient temperature and pressure. The boundary conditions were specified as follows,

$$T|_{t=0,r,z} = T_i \tag{36}$$

where T_i was 25 ℃,

$$P_g\big|_{t=0,r,z} = P_{g,i} \tag{37}$$

where $P_{g.i}$ was 1 atm,

$$S_l|_{t=0,r,z} = S_{l,i} \tag{38}$$

where $S_{l.i}$ was 1,

$$Y_{LiH,t=0,r,z} = Y_{LiH,i} \tag{39}$$

$$Y_{LiOH,t=0,r,z} = 1 - Y_{LiH,i} \tag{40}$$

where $Y_{LiH,i}$ was set to 1,

$$Y_{air,t=0,r,z} = Y_{air,i} \tag{41}$$

$$Y_{H_2,t=0,r,z} = Y_{H_2,i} \tag{42}$$

$$Y_{H_2Og,t=0,r,z} = 1 - Y_{H_2,i} - Y_{air,i} \tag{43}$$

where $Y_{air,i}$ was set to 1 and $Y_{H_2,i}$ was set to 0.

Boundary Conditions

The model does not include the membrane or the water reservoir; instead, a liquid water flux is applied at the inlet boundary. A time dependent water flux was developed and applied at the inlet boundary condition (at $r = R_i$) to represent the membrane dynamics for the liquid water feeding. The time-dependent inlet boundary condition was approximated as follows,

$$\frac{\partial}{\partial x_j}\left(\rho_l u_{j,l}\right)\Big|_{t,r=R_i,z} = \max\left(\dot{m}''_{H_2Ol,max}, \dot{m}''_{H_2Ol,max}\tanh(t/10)\mathrm{e}^{(-0.01*t)}\right) \tag{44}$$

where $\dot{m}''_{H_2Ol,max}$ is the maximum mass flux of liquid water at inlet, t is time. $\dot{m}''_{H_2Ol,max}$ was approximated from the average mass flow rate, $\dot{m}''_{H_2Ol,avg}$, obtained in the experimental runs (see Table 1). For run 1, 2, and 3, $\dot{m}''_{H_2Ol,max}$ was approximated to 0.003 kg/s-m^2, and for run 4, $\dot{m}''_{H_2Ol,max}$ was approximated to 0.013 kg/s-m^2.

The liquid water was assumed to enter the bed at a constant temperature of T_{R_i}:

$$T|_{t,r=R_i,z} = T_{R_i} \tag{45}$$

where T_{R_i} was 25 ℃,

The outlet boundary condition (at $z = L$) is an open boundary that allows for the gas mixture (hydrogen, air, and water vapor) and the liquid water to exit the domain. The radius of the outlet boundary is smaller than the LiH bed radius, R. The axis of symmetry was specified at $r = 0$, and bottom and top surfaces ($z = 0$ and $z = L$) are assumed to be insulated walls.

Procedures

Experiment

Four different experiments were used to validate the numerical model. The experimental setup (Figure 3a) is composed of a water tank, the refueler, a dehumidifier, and a volumetric flow rate meter. The refueler (Figure 3b) consists of two concentric cylinders, and the design parameters are listed in Table 1. The inner cylinder is filled with 0.75 – 1.75 grams of LiH powder (with an average particle diameter of 100 μm), and the outer cylinder is filled with liquid water upon activation of the system. The inner cylinder filled with lithium hydride is separated from the water outer cylinder by a membrane that allows the liquid water to slowly permeate into the LiH porous bed. Hydrogen gas is generated via the reaction of water and LiH. The conduit has a diameter of $D_b = 0.375$ inches and a length of $L = 2.25 - 3.5$ inches. The polycarbonate outer shell of the refueler has an outside diameter of $D_w = 0.75$ inches and a wall thickness of 0.0625 inches, and it is connected upstream to a water tank that feeds liquid water into the outer shell of the refueler. The water tank contained 12.07 milliliters of liquid water. Gravity is used to ensure that the outer shell of the refueler is always filled with liquid water. The inner cylinder of the refueler is connected to a dehumidifier used to remove water vapor from the produced gas mixture exiting

the porous bed. The volumetric flow rate of the gas mixture is measured downstream the dehumidifier with an Omega mass flowmeter.

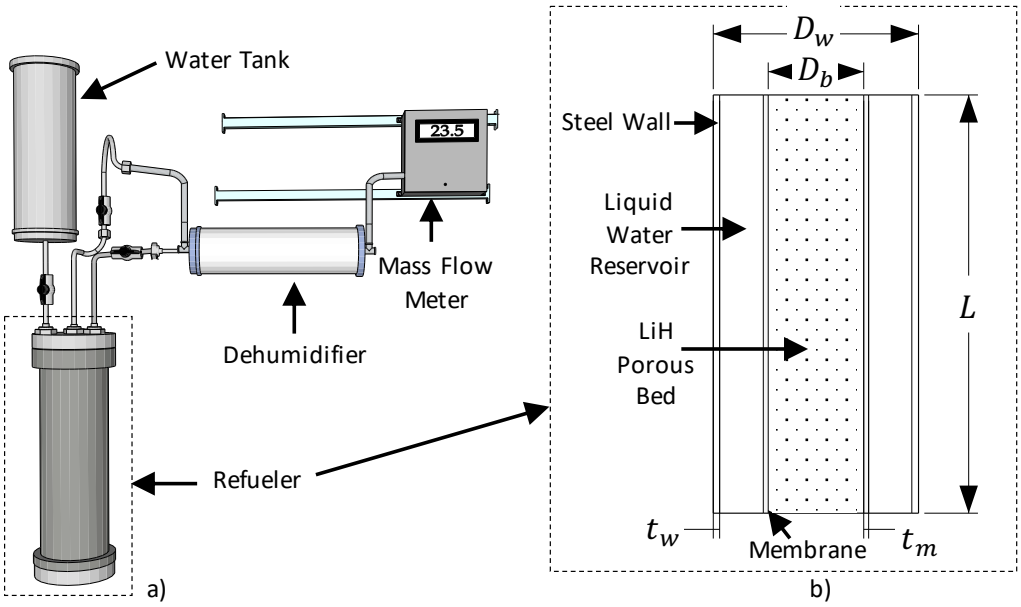

Figure 3: a) Schematic of experimental setup which includes water tank, refuelers, dehumidifier, and mass flow meter, and b) experimental refueler with dimensions.

Table 1: Design parameters of experimental refueler.

Experiment	**Run 1**	**Run 2**	**Run 3**	**Run 4**
Bed diameter (D_b)	9.525 mm (0.375 in)			
Membrane thickness (t_b)	0.127 mm (0.005 in)			
Water tank diameter (D_w)	19.05 mm (0.75 in)			
Water tank thickness (t_b)	1.588 mm (0.0625 in)			
Length (L)	57.15 mm (2.25 in)	76.2 mm (3.0 in)	88.9 mm (3.5 in)	69.85 mm (2.75 in)
Initial LiH mass (m_{LiH})	0.75 g	0.81 g	1.75 g	1.4 g
Average inlet liquid water mass flow rate ($\dot{m}''_{H_2Ol,avg}$)	0.001 kg/s-m^2	0.001 kg/s-m^2	0.001 kg/s-m^2	0.01 kg/s-m^2

It is important to note that the uncertainty of the experimental measurements was mainly driven by the uncertainty of the liquid water mass flow rate at the inlet of the bed. It was not possible to measure the rate at which the liquid water permeates through the membrane. Instead, a constant mass flow rate was estimated by dividing the change in the liquid water volume in the outer cylinder by the time the experiment ended (listed in Table 1). From membrane theory, it is known that the water flux increases with increasing temperature [21].

The temperature was measured for only one of the experiments due to the difficulty of inserting the thermocouple into the LiH bed without damaging the membrane. In addition, having the thermocouple inside of the bed disrupts the reaction and the uniform porosity of the bed increasing the uncertainty of the experimental results. The thermocouple was placed at the center of the LiH

bed (at $L/2$ and $D_b/2$). The thermocouple was rated for a maximum temperature of 300 degrees Celsius, so there were no accurate measurements once the temperature of the bed exceeded 300 degrees Celsius. At the end of this run, it was observed that the membrane had been damaged. The damage on the membrane could have been caused by either the expansion of the solid when LiOH was formed, by thermal degradation due to the rapid increase in temperatures, or by the insertion of the thermocouple. The damaged membrane allowed water to enter the LiH bed freely which rendered the measurements of hydrogen flow rates unreliable. The temperature measurements were still used to validate the model. The mass flow rate for this run was one order of magnitude higher than the mass flow rate for the rest of the runs.

Numerical Model

A Sandia-developed code called Sierra:Aria was used to perform the simulations [22]. Aria [23] is a Thermal/Fluids Multiphysics finite element software suite that performs steady and unsteady thermal analysis of 2D or 3D systems. In this work, a 2D axis-symmetric computational domain of a cylindrical LiH conduit (see Figure 2) was used to solve for the coupled partial differential equations listed in the Introduction-Governing Equations section. The mesh has a total of 6744 nodes. The mesh was refined closer to the outlet boundary to avoid any instabilities.

The thermal properties of liquid water, LiH, and LiOH were assumed constant, and are listed in Table 2. The thermal properties of hydrogen, air, and water vapor vary with temperature and were obtained from NIST [24].

Table 2: Thermal Properties of species in the system.

Property	LiH	$LiOH$	H_2	H_2Ol	H_2Og	Air
Molecular Weight (g/mol)	7.948	23.94	2.015	18.02	18.02	28.97
Density (kg/m^3)	780	1460	Ideal Gas	997.0	Ideal Gas	Ideal Gas
Specific Heat (J/g-K)	3510.0	2070.0	NIST	4184.0	NIST	1000
Thermal conductivity (W/m-K)	12.5	0.65	NIST	0.607	NIST	25.72E-3
Viscosity ($Pa-s$)	-	-	NIST	1.753E-3	NIST	1.81E-5
Enthalpy of reaction (kJ/mol)	-90400	-487500	-	-285820	-241820	-
Mass Diffusivity (m^2/s)	-	-	4.0E-7	4.50E-9	7.8E-9 [10]	2.82E-5

The values used for the Arrhenius equation (see Equation (6)) for Reaction (1) and (2) are listed in Table 3.

Table 3: Values for Arrhenius reaction rate equation for reaction (1) and (2).

Parameter	Reaction (1) [7]	Reaction (2) [25]
A	1.72E-6 s^{-1}	-
E_a	-6700 J/mol	-
k_j	-	0.0044
n	1.0	1.3
m	1.0	0.25

A parametric study was performed to determine the effects of varying design parameters on the hydrogen generation and the temperature in the lithium hydride bed. A reference case scenario was used as the starting point for the parametric study, specifically Experimental run 1. The inlet mass

flux of liquid water was kept constant in the parametric study, where $\dot{m}''_{H_2Ol,max} = 0.003\,\mathrm{kg/(m^2 s)}$ was used.

The parameters varied from the reference study were:

1. initial temperature of the LiH bed,
2. inlet temperature of the liquid water,
3. diameter of the bed with constant initial lithium hydride mass,
4. diameter of the bed with constant porosity,
5. length of the bed with constant initial lithium hydride,
6. length of the bed with constant porosity, and
7. initial mass of lithium hydride in the bed.

The parameters used for the reference case scenario as well as the range used for each parameter are shown in Table 4.

Table 4: Parametric study values.

Parameter	Reference Case	Range
initial temperature of the LiH bed, T_i (°C)	25	2 – 50
inlet temperature of the liquid water, T_{R_i} (°C),	25	2 – 50
diameter of the bed with constant initial LiH mass, R_i (in)	0.375	0.2 – 0.5
diameter of the bed with constant porosity, R_i (in)	0.375	0.2 – 0.5
length of the bed with constant initial LiH mass, L (in)	2.75	2 – 5
length of the bed with constant porosity, L (in)	2.75	2 – 5
initial mass of lithium hydride in the bed, $m_{LiH,t=0}$ (kg)	1.4	0.25 – 2

For presentation purposes, the parameters in Table 4 were normalized to have a range of 0 to 1 as follows:

$$n = \frac{a - a_{min}}{a_{max} - a_{min}} \quad \text{for } a = T_{R_i}, T_{r=R_i}, R_i, L, m_{LiH,t=0} \tag{46}$$

where the minimum (a_{min}) and maximum (a_{max}) values are obtained from the lower and upper limits of the range listed in Table 4.

Results and Discussion

Validation

The results from the four experiments run by Skyhaven were used to validate the numerical model. The dimensions and initial LiH mass listed in Table 1 were used for the numerical model. The validation effort consisted of calibrating the mass flow rate of water at the inlet boundary condition, and the temperature at the center of the bed. Experimental runs 1, 2, and 3 were used for the mass flow rate validation only since no temperature measures were performed. Experimental run 4 was used for the temperature validation only since the mass flow rate measurements were not correctly recorded due to the fracture in the membrane.

Figure 4 shows the comparison between experimental and numerical results for the outlet mass flow rate of hydrogen. The numerical model is able to predict the general behavior of the mass flow rate of hydrogen leaving the bed. The model does a good job of reproducing the mass flow rate until the maximum is reached. Once the maximum is reached, the numerical results start deviating from the experimental results. This is most likely due to the decrease in the permeability of the bed due to the formation of the LiOH solid layer. The permeability in the model is calculated using Equation (22), where the particle diameter of LiH and LiOH are used. In the model, the particle diameter of LiH and LiOH is assumed to be constant, when in reality, the particle diameter of both LiH and LiOH changes with time. In addition, since the model is not solving for the water flux through the membrane and a time dependent water flux approximation was developed to be applied at the inlet boundary condition (at $r = R$), some of the dynamics happening in the membrane from pressure changes in the LiH bed are most likely not captured by time-dependent approximation, which would result in a different outlet hydrogen mass flow rate.

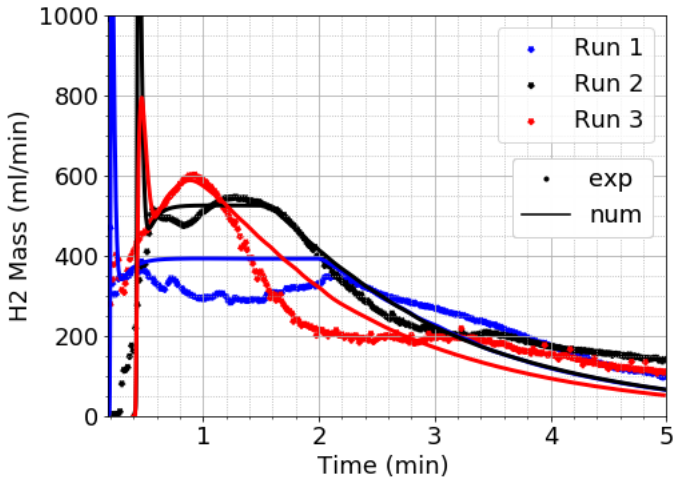

Figure 4: Comparison between experimental and numerical results for the outlet mass flow rate of hydrogen gas of run 1, 2, and 3 (see Table 1).

Figure 5 shows the comparison between the experimental and numerical temperature at the middle of the bed. The numerical model does a good job at predicting the temperature rise inside of the bed, and it predicts a maximum temperature of 400 °C. It is important to note that the membrane fractured in this experimental run, water was able to flow in more freely than in run 1, 2, and 3. This resulted in a higher hydrogen outlet mass flow rate and a higher temperature than observed in experimental 1, 2, and 3. Run 4 had an inlet water mass flow rate almost an order or magnitude greater than the one observed in runs 1,2, and 3.

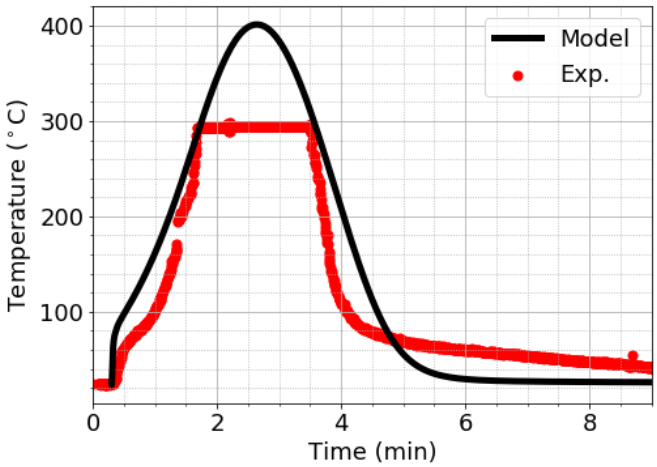

Figure 5: Comparison between the experimental and numerical temperature at the middle of the bed for Experimental run 4. The numerical model faithfully predicts the temperature rise inside of the bed.

Results

The inlet mass flow rate was varied in order to determine its effect on the temperature inside of the bed. Specifically, $\dot{m}_{H_2Ol,max}$ in Equation (44) was varied from 0.008 kg/m^2-s to 0.015 kg/m^2-s. Figure 6 shows the temperature at the middle of the bed as a function of time using parameters for experimental run 4. The LiH bed temperature significantly decreases as the inlet liquid water mass flow rate decreases. The temperature of the bed decreases 100 °C when the mass flow rate is decreased to almost half its value. By reducing the inlet mass flow rate, the reaction slows down, but if the same amount of water is fed into the bed, the toal amount of hydrogen generated at the end of the process will remain almost contant. It was also observed that slowing down the reaction, can also be beneficial to achieve closer to 100% LiH reaction conversion because water is able to reach more LiH before the LiOH is formed and decreases the water permeation. For the emergency refueler, the reaction cannot be slowed down too much because it still needs to be able to produce enough hydrogen for the customer in less than 15 minutes. The mathematical model demonstrates the importance of a controlled water feed to the LiH bed to maintain a stable LiH bed temperature and prevent thermal runaway. The numerical model further demonstrates that decreasing water flux decreases maximum temperature while maintaining an overall hydrogen production.

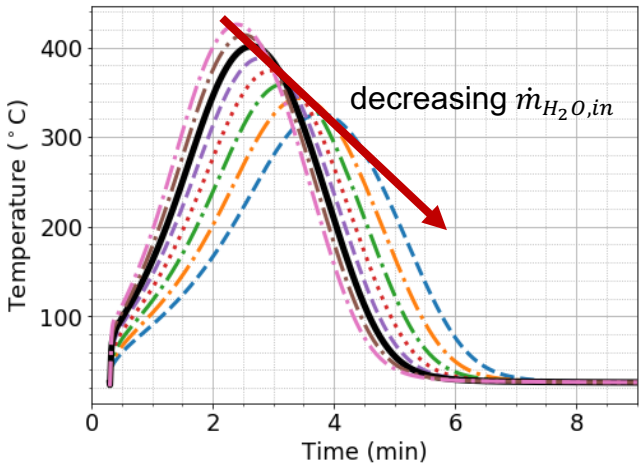

Figure 6: Temperature at the middle of the bed as a function of time using parameters for experimental run 4.

Figure 7a) shows the minimum porosity as a function of the seven normalized parameters. The minimum porosity is the same for all the cases except for the case where the diameter and length of the bed were varied with a constant initial LiH mass, and where the initial mass of LiH in the bed was varied. As the diameter of the bed decreases, the minimum porosity approaches zero which indicates that water is not able to flow to the rest of the bed.

Figure 7b) shows the maximum pressure inside of the bed as a function of the seven normalized parameters. A maximum pressure exceeding 10 MPa is observed for the bed with the smallest diameter and a porosity of 0.19. Since the porosity is very low, liquid water is able to permeate the bed easily and reaches more of the LiH before the LiOH layer starts forming and obstructs water to permeate further. The outlet of the bed is not sufficiently large to quickly release the hydrogen being produced to lower the pressure of the bed. In addition, once the LiOH layer starts forming, the porosity decreases to the point where the water and gas will not be able to leave the bed, resulting in an increase of pressure. Note that in the real system, the membrane decreases the mass flow rate going into the system in order to stabilize the pressure in the bed. In this model, the membrane is not being modeled, and this effect is not captured. A similar effect is observed in the case where the initial LiH increases (yellow-dashed-dot line). As the initial LiH increases, the initial porosity decreases (as shown in Figure 7a)). As porosity decreases, the pressure in the bed starts increasing. For the rest of the cases, the pressure remains almost constant. This is because the bed is able to release the produced hydrogen at the rate needed to maintain the pressure low.

Figure 7c) shows the total hydrogen produced by the LiH bed as a function of the seven normalized parameters. As expected, there was no change in the total hydrogen produced when the inlet or initial temperatures are varied. There was also no change for the case where the initial LiH mass was increases. This is because $\dot{m}''_{H_2Ol,max}$ in Equation (44) was kept constant during the parametric study, so even though there was more LiH to react with water, the amount of water fed to the bed was the same. An improvement on the hydrogen production was shown for the cases where the geometry was modified, namely the diameter and length (both case 1 and 2). The reason for this is that when the diameter or the length is increased (surface area also increases), the total amount of water fed to the bed increases. There is more water to react with the LiH. One important aspect

of the model is that the water flux that going into the bed is the same, so for some cases there won't be enough water to reach 100% LiH reaction conversion.

Figure 7d) shows maximum temperature of the bed as a function of the seven normalized parameters. The maximum temperature of the system can significantly be reduced if the inlet or initial temperature are below 2 °C. Even though there is a significant decrease in the maximum temperature in the bed if the initial or inlet temperature are at 2 °C, it is not recommended to design the refueler at this low temperature since freezing of water can occur. The model did not take into account water freezing. Except for the 2 °C, there was no significant advantage of changing the inlet or initial temperature of the bed. On the other hand, a minimum on the maximum temperature was observed for the case where the diameter of the bed was increased while maintaining the LiH mass constant (changing porosity). Specifically, the minimum temperature decrease (only 5 °C decrease) was observed at $R_i = 0.23$. As the diameter decreases, a sharp increase in the maximum temperature can be observed. For $R_i = 0.2$ in, the temperate increased 46 °C. This increase in temperature is mainly driven by the increase in pressure in the system. As mentioned before, when the diameter is small, the porosity decreases so much that the liquid water and the gas mixture cannot reach the outlet of the bed. Increasing the length of the bed resulted in the best results. When the length of the bed is increased, the temperature is maintained low as the production of hydrogen is increased.

The parametric study shows that lower liquid water inlet flow rates resulted in a more stable hydrogen production and a lower temperature in the refueler. The model also predicts that the inlet water temperature of the bed has no effect on the maximum temperature of the bed because the heat of reaction predominates. Longer reactors exhibit higher LiH reaction conversion and lower maximum temperature.

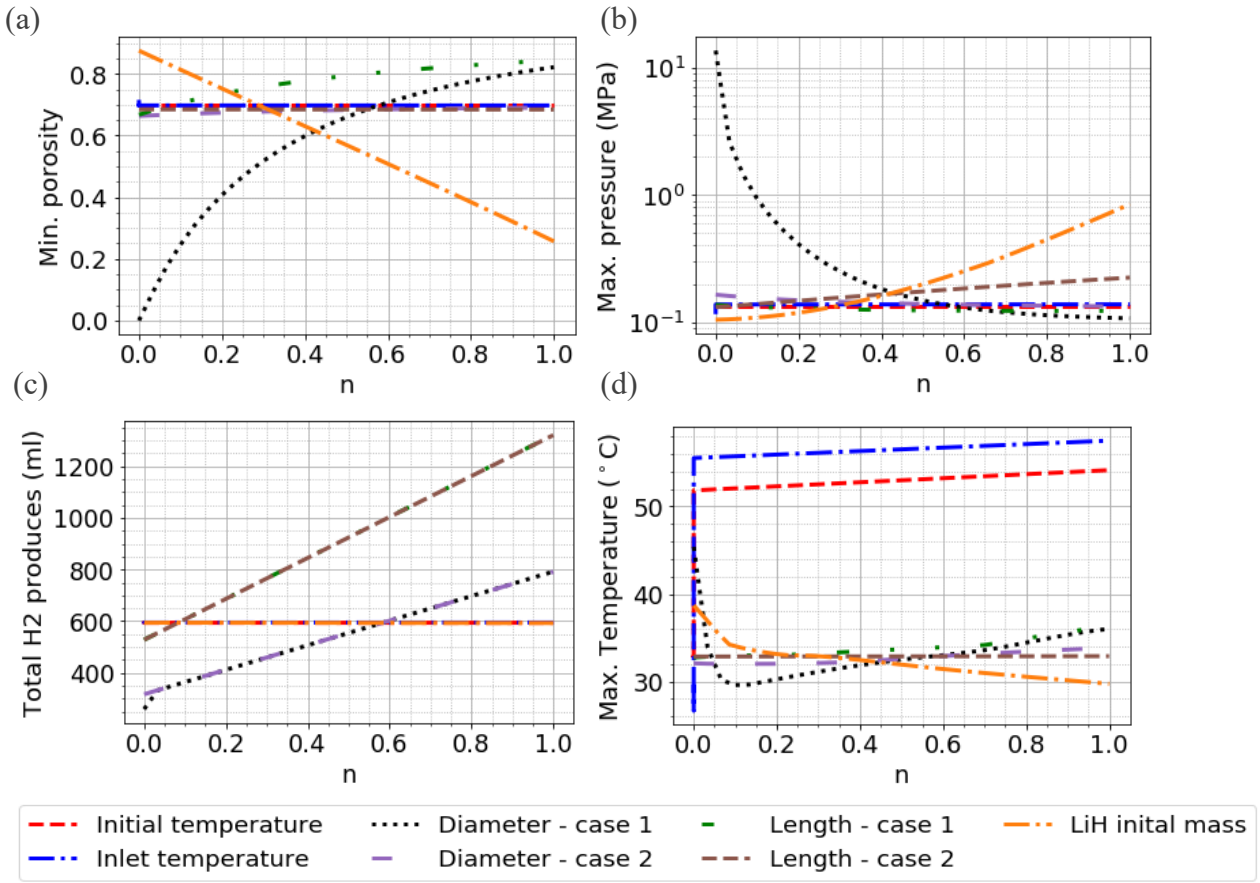

Figure 7: a) Maximum porosity, b) maximum pressure, c) total hydrogen produced, and d) maximum pressure as a function of normalized: initial temperature of the LiH bed, inlet liquid water temperature, diameter of the bed with constant initial mass of LiH, diameter of bed with constant initial porosity, length of the bed with constant initial mass of LiH, length of bed with constant initial porosity, and initial LiH mass.

Implementation

Technical Objectives

The technical goal is to develop a robust Multiphysics model of the refueler reactor that will be used to improve the design and performance of the current refueler prototype. Specifically, the following performance goals need to be achieved:

1. 100% LiH reaction conversion within 15 minutes
2. Maximum pressure inside the reactor bed below 2,000 psia
3. Temperature inside the reactor bed below 100 degrees Celsius
4. Reduce the reactor's mass and volume

Phases of the Project

This project was split into three phases. The first phase was the development a single cell model of the hydrogen refueler, conducting validation testing, and conducting parametric studies. The second phase was the expansion of the single cell model to a multi-cell model of the hydrogen refueler, which included conducting validation testing and parametric studies. The third phase was to prepare and deliver a final report.

Due to the changes in the refueler design and operation, phase two was replaced by incorporating the new physics and mesh modification to the model from phase 1.

TASKS	MILESTONES	COMPLETED
1- Single Cell Model Development	Computational model of a single-cell unit of the refueler, accounting for • conservation of mass • conservation of momentum • conservation of energy • radial and axial spatial dimensions • transient operation	✓
2- Single Cell Validation Testing	Validation of the single cell model to measured single cell performance data to include • H_2 delivery rate over time • Thermal distribution over time • Pressure over time	✓
3: Single Cell Parametric Studies	Execution of the model to identify design parameters that optimize the single cell reactor focusing on • 100% LiH reaction conversion within 15 minutes • Pressure generation up to 2000 psia • Internal temperature distribution less than 100 °C • Minimal mass • Minimal volume	✓
4- Multi Cell Model Development	Computational model of a multi-cell refueler that encompasses the single cell model from Tasks 1-3, accounting for • Internal heat transfer fins between single cells • External heat transfer fins	⃠ Replaced with adding new physics for new design
5:Multi-Cell Validation Testing	Validation of the multi-cell model to measured multi-cell performance data to include • H_2 delivery rate over time • Thermal distribution over time • Pressure over time	⃠ Replaced with validating new model from task 4.

6: Multi-Cell Parametric Studies	Execution of the model to identify design parameters that optimize the multi-cell refueler focusing on • 100% LiH reaction conversion within 15 minutes • Pressure generation up to 2000 psia • Internal temperature distribution less than 100 °C • Minimal mass • Minimal volume	⃠ Replaced with parametric study using new model from task 4
7: Writing Report		✓

Issues or Challenges

The main challenges of this project were:

1. the addition of liquid water to the system
2. unknown inlet mass flow rate of liquid water
3. changing diffusivity of the liquid and gases on a LiH and LiOH bed
4. changing permeability of the bed
5. the Van Genuchten parameters
6. rapid reaction rate of liquid water with LiH

Modeling the addition of liquid water to the system required the extension the model with two-phase flow theory. The Van Genuchten parameters, n and α, in Equations (15) needed to be obtained experimentally for the system that is being considered. This was not part of the scope for Skyhaven's project, and we were unable to find these parameters specifically for LiH and LiOH in the literature. Instead, the parameters for a soil called "L-soil" given by Webb [3] were used in the model, and they were assumed to be constant. However, the Van Genuchten parameters are not constant for the LiH and LiOH bed because they change as LiH reacts with water to form LiOH. Phase change was also introduced, which makes the differential equations in the model numerically stiffer.

Since the inlet mass flow rate of water was unknown, a time-dependent expression was derived to reproduce the experimental results. The diffusion coefficients of the liquid and gases were assumed to be constant, and values from literature were used. The permeability of the bed was assumed to be a function of the particle diameter of LiH and LiOH and mass fractions of LiH and LiOH. The particle diameter of LiH and LiOH were assumed constant. Skyhaven was not able to measure the reaction of liquid water with LiH because it finishes too quickly. Instead, we relied on values found in the literature.

Difficulties encountered while running the validation experiments, added additional uncertainties to the experimental data, making validation of the model more challenging. The validation effort took longer than expected because determining reliable boundary conditions for the model required delicate control of experimental measurements. We discussed this with Skyhaven, and Skyhaven agreed to run a new set of experiments where both temperature and hydrogen mass flow rate were going to be measured. However, these experiments were unexpectedly postponed indefinitely as a result of the COVID-19 pandemic.

Impact

Company Impact: Describe the economic, energy, and/or material consumption impacts your company expects to realize due to this project. Impact examples include energy and material savings, increased competitiveness, job creation or enhanced job stability.

Describe how collaborating with the National Laboratories has impacted your organization's operations and competitiveness. Descriptions can be qualitative or quantitative in nature as appropriate.

This collaboration enables the development of a numerical model that helped improve the emergency refueler design from Skyhaven helping the U.S. The technical challenges were beyond the modeling capabilities of Skyhaven, so it was informative to work with Sandia's experts on how they approach such challenging modeling environments. Numerous technical discussions between Sandia and Skyhaven kept evolving the refueler design and modeling approach leading to a better system ultimately.

National Impact: Describe how the results of this project can or will lead to national scale impacts. What economic, energy, and/or material impacts be to your industry? Examples include energy and material savings, increased competitiveness, job creation or enhanced job security or stability.

Offering this emergency hydrogen refueler to vehicle owners will help alleviate range anxiety, accelerate the commercialization of hydrogen fuel cell vehicles, and promote the continuing commissioning of hydrogen refueling stations. This early-research and development project supports the nation's energy strategy—helping to diversify America's energy sector, reduce the dependence on foreign oil, and help reduce petroleum combustion emissions by accelerating the deployment of fuel cell vehicle technologies. The hydrogen refueler will greatly reduce barriers to market penetration by allowing hydrogen fuel cell vehicle users an extended driving range in case of emergency due to a lack of hydrogen refueling stations. This project will contribute to the goal of advancing hydrogen and fuel cells for transportation and diverse applications which contribute to U.S. energy independence, security and resiliency, and add to a strong domestic economy for taxpayers.

Future Work

The model was not able to fully reproduce the experimental results because there were too many unknowns. These unknowns include:

1. the Van Genuchten parameter for LiH and LiOH porous bed,
2. the permeability of the bed as the LiOH layer forms,
3. the mass diffusivity of the gas and liquid phase species as the LiOH layer forms, and
4. the liquid water inlet mass flow rate.

The saturation and capillary pressure parameters (Van-Genuchten parameters) for a LiH/LiOH system with a two-phase flow should further be explored. Experiments need to be conducted to measure the capillary pressure and saturation for solids. From these measurements, the Van Genuchten parameters can be obtained. This is a difficult task since the Van Genuchten parameters change as the LiH reacts with water to produce LiOH and hydrogen. An alternative to this approach is to calibrate Van Genuchten parameters in the model using more experimental data.

In order to improve the agreement between the numerical and experimental results, the membrane should be characterized experimentally, and also added to the numerical model. This would eliminate the reliance on the approximated time-dependent inlet mass flux in Equation (44). In addition, more experiments should be performed in order to collect more temperature data. The diffusion models should be improved to better capture the decrease in water permeating in the bed due to the formation of a LiOH-H_2O film.

Pictures for Publication:

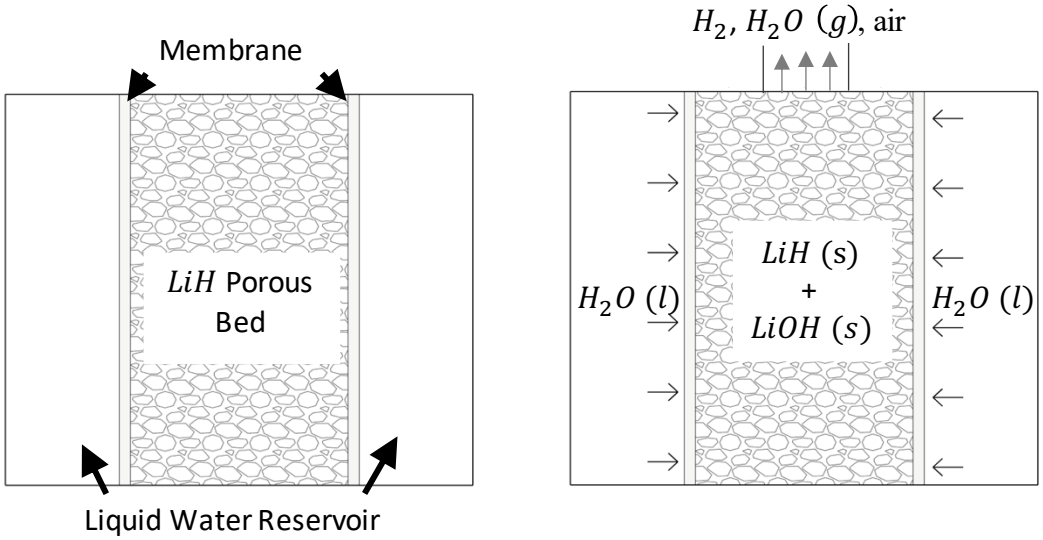

Hydrogen refueler consists of a cylindrical conduit filled with LiH powder. Liquid water permeates through the conduit wall and immediately reacts with LiH particles to produce hydrogen and LiOH.

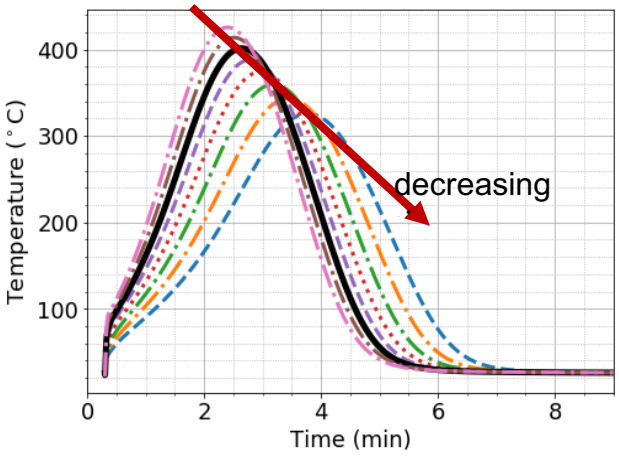

Temperature at the middle of the bed as a function of time for varying inlet mass flow rate. The LiH bed temperature significantly decreases as the inlet liquid water mass flow rate decreases.The mathematical model demonstrates the importance of a controlled water feed to the LiH bed to control LiH bed temperature and prevent thermal runaway.

Laboratory PI Experience Feedback

(1) Why were you interested in working with the HPC4EI Program?

I have been previously involved in the hydrogen group at Sandia National Labs, where I used my expertise on heat transfer and fluid dynamics to model hydrogen releases. I also have expertise on modeling reactive flows in porous media, so I found the proposal of Skyhaven very interesting and within my area of expertise. BHPC4Materials gave me the opportunity to collaborate with a company outside Sandia, which has been a learning experience for me. This program allowed me to focus on the modeling of this complex system, and leverage Sandia's tools to solve impactful research questions. HPC4Materials also gave me the opportunity to learn about the research other labs and companies are doing in different fields.

(2) Was your overall experience as part of the HPC4EnergyInnovation Program positive, neutral, or negative? Why?

My experience was positive overall. I did face modeling challenges due to the change in the refueler's design as well as the lack of material model characterization of the system. The validation effort took longer than expected because the experimental measurements needed to be more controlled in order to have better boundary conditions for the model. We discussed this with Skyhaven, and Skyhaven agreed to run a new set of experiments where both temperature and hydrogen mass flow rate were going to be measured. Unfortunately, these experiments could not be completed due to the COVID-19 pandemic.

(3) Did your experience as an HPC4EI PI help build your capabilities and expertise? How?

Sandia was able to improve the physics models of complex systems such as the refueler. SNL validated the model against experimental data produced by Skyhaven. SNL will be able to use this type of models for projects that deal with similar physics, such as thermal batteries. In addition, SNL was able to expand Sierra's material property library with data provided by Skyhaven.

I was able to expand my expertise on two-phase flow. Having two-phase flow was not part of the project initially. However, the design of the refueler changed to have liquid water (instead of water vapor) react with LiH. By introducing liquid water to the system, we needed to add two-phase flow and phase change equations to the model. I had no previous experience modeling two-phase flows, and now I can include that as part of my skillset.

(4) How can the HPC4EnergyInnovation program be improved?

One thing that I struggled with being part of this program was not knowing who to reach out to when I had programmatic issues. When the design of the refueler changed, I had to add the new physics to the model and change the domain and boundary conditions. This delayed my progress on the deliverables I had agreed to. Looking back, I should have probably reached out to the program managers to discuss the changes and how they were going to affect the project deliverables. Instead, I agreed to the changes and still tried (unsuccessfully) to meet all the deliverable timelines. I ended up reducing the scope of the project due to the 1-year restraint. Two things that could be improved:

1. Give a clear descriptions of what the expectations are for the program to both the Lab and the industry PIs.
2. Have a point of contact that PIs can reach out to in case there is an issue PIs need to resolve.

Company Experience Feedback

(1) Have you already or do you intend to submit a Phase 2 proposal for this project?

a. If yes, when?

b. If no, why not? There is no intention of submitting a follow-on proposal for modeling the hydrogen refueler. There are sufficient results from the Phase I modeling work to provide some insight into the hydrogen refueler operation. On-going development work at Skyhaven on the hydrogen refueler continues to evolve the design and operation of the refueler, and with such dynamic changes underway it is not really amenable to a modeling effort that would be better served via a fixed design.

(2) Is this your first project funded through the HPC4EnergyInnovation Program? If not, with how many previous projects have you been involved?

This is Skyhaven's first project with the HPC4EnergyInnovation Program.

(3) Was your overall experience as part of the HPC4EnergyInnovation Program positive, neutral, or negative? Why?

The overall experience for Skyhaven working with Sandia on this program was positive. The refueler has a high level of technical complexity including transient operation, transient and spatially changing porous media, reactive flows, two-phase flow, and heat transfer. These technical challenges are beyond the modeling capabilities of Skyhaven, so it was informative to work with Sandia's experts on how they approach such challenging modeling environments. Numerous technical discussions between Sandia and Skyhaven kept evolving the refueler design and modeling approach leading to a better system ultimately.

(4) Are you interested in working with one or more HPC4EI affiliated laboratories on one or more future HPC4EI projects? On one or more future projects outside of the HPC4EI Program?

Skyhaven is open to future collaborations with HPC4EI affiliated laboratories for other projects the firm is conducting. The firm continues to innovate on a number of DOE funded projects via the SBIR program, where upon conducting a Phase II SBIR program the firm would be amenable to discussing how HPC4EI modeling initiatives can further advance the technology to support the firm's commercialization of the product.

(5) How can the HPC4EnergyInnovation Program be improved or augmented to better serve your needs?

No substantive changes are needed for the HPC4EnergyInnovation Program. Skyhaven found the programmatics easy to execute, although the technology solutions were very

difficult to implement. This was a good example of a government-industry partnership where programmatic and contractual details did not get in the way of progress, thus enabling the teams to focus on the challenging technical development.

References

1. Van Genuchten, M., *Calculatingthe Unsaturated Hydraulic Conductivity with a New Close-Form Analytical Model.* Res. Rep, 1978.
2. Van Genuchten, M.T., *A closed-form equation for predicting the hydraulic conductivity of unsaturated soils 1.* Soil science society of America journal, 1980. **44**(5): p. 892-898.
3. Webb, S.W., *A simple extension of two-phase characteristic curves to include the dry region.* Water Resources Research, 2000. **36**(6): p. 1425-1430.
4. DOE, *Fuel Cell Technologies Program Multi-Year Research, Development, and Demonstration Plan*. 2007, US Department Of Energy Washington, DC.
5. Kong, V., et al., *Development of hydrogen storage for fuel cellgenerators. i: Hydrogen generation using hydrolysishydrides.* International Journal of Hydrogen Energy, 1999. **24**(7): p. 665-675.
6. Dinh, L., et al., *The nature and effects of the thermal stability of lithium hydroxide.* Journal of nuclear materials, 2003. **317**(2-3): p. 175-188.
7. Haertling, C., R. Hanrahan Jr, and R. Smith, *A literature review of reactions and kinetics of lithium hydride hydrolysis.* Journal of nuclear materials, 2006. **349**(1-2): p. 195-233.
8. Mazumder, S. and J.V. Cole, *Rigorous 3-D mathematical modeling of PEM fuel cells: II. Model predictions with liquid water transport.* Journal of the Electrochemical Society, 2003. **150**(11): p. A1510.
9. Natarajan, D. and T. Van Nguyen, *A two-dimensional, two-phase, multicomponent, transient model for the cathode of a proton exchange membrane fuel cell using conventional gas distributors.* Journal of the Electrochemical Society, 2001. **148**(12): p. A1324.
10. Nguyen, T. and R.E. White, *A finite difference procedure for solving coupled, nonlinear elliptic partial differential equations.* Computers & chemical engineering, 1987. **11**(5): p. 543-546.
11. Springer, T.E., T. Zawodzinski, and S. Gottesfeld, *Polymer electrolyte fuel cell model.* Journal of the electrochemical society, 1991. **138**(8): p. 2334.
12. Mualem, Y., *A new model for predicting the hydraulic conductivity of unsaturated porous media.* Water resources research, 1976. **12**(3): p. 513-522.
13. Darcy, H.P.G., *Les Fontaines publiques de la ville de Dijon. Exposition et application des principes à suivre et des formules à employer dans les questions de distribution d'eau, etc*. 1856: V. Dalamont.
14. Welty, J.R., et al., *Fundamentals of momentum, heat, and mass transfer*. 2009: John Wiley & Sons.
15. Bruggeman, V.D., *Berechnung verschiedener physikalischer Konstanten von heterogenen Substanzen. I. Dielektrizitätskonstanten und Leitfähigkeiten der Mischkörper aus isotropen Substanzen.* Annalen der physik, 1935. **416**(7): p. 636-664.
16. Um, S., C.Y. Wang, and K. Chen, *Computational fluid dynamics modeling of proton exchange membrane fuel cells.* Journal of the Electrochemical society, 2000. **147**(12): p. 4485-4493.
17. Carman, P.C., *Fluid flow through granular beds.* Trans. Inst. Chem. Eng., 1937. **15**: p. 150-166.
18. Carman, P.C., *Permeability of saturated sands, soils and clays.* The Journal of Agricultural Science, 1939. **29**(2): p. 262-273.
19. Kozeny, J., *Soil permeability.* Sitzungsber. Oesterr. Akad. Wiss. Wien. Math. Naturwisss. Kl. Abt, 1927. **136**: p. 271.
20. Luckner, L., M.T. Van Genuchten, and D. Nielsen, *A consistent set of parametric models for the two-phase flow of immiscible fluids in the subsurface.* Water Resources Research, 1989. **25**(10): p. 2187-2193.
21. Fathima, N.N., et al., *SPEEK polymeric membranes for fuel cell application and their characterization: A review.* 2007.

22. Williams, A.B., *SIERRA Framework Version 4: Solver Services*. 2005, Sandia National Laboratories.
23. Notz, P.K., et al., *SIERRA Multimechanics Module: Aria User Manual – Version 4.40*. 2016, Sandia National Laboratories.
24. Lemmon, E.W., M.L. Huber, and M.O. Mclinden, *NIST standard reference database 23: reference fluid thermodynamic and transport properties-REFPROP, version 8.0.* 2007.
25. Prosini, P.P., C. Cento, and P. Gislon, *Steam hydrolysis of lithium hydride.* International journal of green energy, 2010. **7**(1): p. 103-115.